IWW

International Wigner Workshop 2023

Book of Abstracts

June 11-12, 2023

Casa Convalèscencia, Barcelona, Spain

www.iww-meeting.info/iww2023/

Hosted by

International Workshop on Computational Nanotechnology (IWCN) 2023

Edited by

Stefano Olivares
Josef Weinbub

ISBN 978-3-9504738-5-8

Supported by

Wigner Initiative
www.iue.tuwien.ac.at/wigner-wiki/

Institute for Microelectronics, TU Wien
www.iue.tuwien.ac.at

Welcome to the *International Wigner Workshop (IWW) 2023*, being held on June 11-12, 2023 at the Casa Convalèscencia, Barcelona, Spain and is hosted by the *International Workshop on Computational Nanotechnology (IWCN) 2023*. The workshop continues to bring together researchers from all areas of science and engineering areas in which Wigner functions have been or could be applied.

IWW 2023 marks the fifth instalment of the International Wigner Workshop series (see www.iww-meeting.info for the full history) and further fosters the growing Wigner Initiative community (www.iue.tuwien.ac.at/wigner-wiki/). The speakers at this year's workshop provided an abstract which was reviewed by the program committee. Topics of interest related to the use of Wigner functions are (but not limited to): Computational or Numerical Challenges, Nanoelectronics, Nanostructures, Quantum Circuits, Quantum Information Processing, Quantum Optics, Quantum Physics, and Quantum Transport.

IWW 2023 hosts five invited and 16 regular speakers, with a total of 31 registered participants.

We would like to express our gratitude to Xavier Oriols (General Chair of IWCN 2023) for supporting our satellite event as well as the participants of IWW 2023 who will make the workshop both interesting and successful. We hope that you enjoy it.

Stefano Olivares and Josef Weinbub
Chairs of IWW 2023
June, 2023

General Chair

Stefano Olivares, *University of Milan, Italy*

Co-Chair

Josef Weinbub, *TU Wien, Austria*

Program Committee

Wolfgang Belzig, *University of Konstanz, Germany*
David K. Ferry, *Arizona State University, USA*
Irena Knezevic, *University of Wisconsin-Madison, USA*
Mihail Nedjalkov, *TU Wien, Austria and Bulgarian Academy of Sciences, Bulgaria*
Franco Nori, *RIKEN, Japan*
Xavier Oriols, *Autonomous University of Barcelona, Spain*
Siegfried Selberherr, *TU Wien, Austria*

Program

Sunday, June 11

8:30 Registration opens in main entrance of “Casa Convalescencia”

Workshop room: *Aula 11-13, on the first floor*

9:00 *Opening Remarks*

Stefano Olivares and Josef Weinbub

9:10 *Optics and Electrodynamics*

Chair: Irena Knezevic

10:50 *Coffee*

16:40 **Invited:** "Minimum uncertainty states with Wigner: quantum hydro-thermodynamics," Nezihe Uzun, *Polish Academy of Sciences* *21*

17:20 "Overcoming the numerical sign problem in the Wigner dynamics via adaptive particle annihilation," Yunfeng Xiong, *Beijing Normal University* *22*

17:40 "Towards the intuitive understanding of the quantum world: Sonification of Wigner function," Reiko Yamada, Eloy Pinol Jimenez, and Maciej Lewenstein, *ICFO – The Institute of Photonic Sciences and ICREA* *24*

20:00 *Reception at restaurant "Ca la Nuria" (close to "Plaça Catalunya")*

Monday, June 12

9:00 *Condensed Matter and Transport* *2*

Chair: David K. Ferry

9:00 "Investigation of a staggered grid formulation of the Wigner transport equation for complex band structures," Mathias Pech, Alan Abdi, and Dirk Schulz, *TU Dortmund* *26*

9:20 "Operational phase-space distribution functions through consecutive weak and strong measurements," Xavier Oriols and Carlos F. Destefani, *Universitat Autònoma de Barcelona* *28*

9:40 Coffee

The Wigner Formalism in High-Energy Quantum Electrodynamics

Christian Kohlfürst

Helmholtz-Zentrum Dresden Rossendorf e.V., Bautzner Landstraße 400,

D-01328 Dresden, Germany

c.kohlfuerst@hzdr.de

We give an overview of the Heisenberg-Wigner phase-space formalism in the context of quantum field theory, in particular strong-field quantum electrodynamics. We discuss the fundamental differences between the Wigner formalism in field theory as compared to the quantum mechanical variant. Most importantly, there is no conservation of the number of particles, thus allowing us to study, for example, electron-positron pair production. In this context, we also show how this high-energy variant of the formalism can be related to low-energy notions, such as the Vlasov equation. Finally, we present some recent developments in the field, both analytically and structurally, as well as numerically.

[1] M. Diez, R. Alkofer, C. Kohlfürst, arXiv:2211.07510 [hep-ph]

[2] C. Kohlfürst, N. Ahmadiniaz, J. Oertel, R. Schützhold, Phys. Rev. Lett. **129**, 241801 (2022)

[3] I.A. Aleksandrov, C. Kohlfürst, Phys. Rev. D **101**, 096009 (2020)

[4] C. Kohlfürst, Phys. Rev. D **101**, 096003 (2020)

[5] C. Kohlfürst, Phys. Rev. D **99**, 096017 (2019)

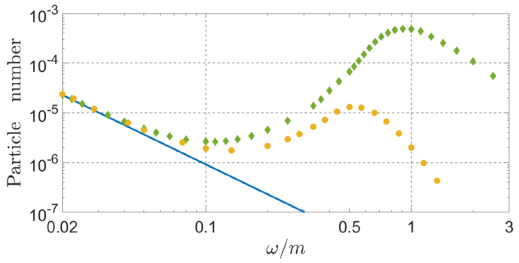

Fig.1: Plot of the mean number of created particles as a function of ω for the profile $E_{cr}t/6\ \exp(-\omega^2t^2)$. The orange circles denote the results of the Dirac-Heisenberg-Wigner formalism in comparison to simple approximations.

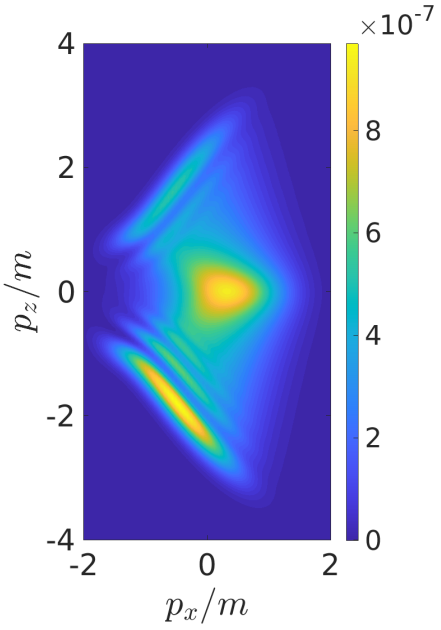

Fig.2: Momentum spectrum of electrons and positrons produced in vacuum by a strong, slowly varying electromagnetic field (Schwinger effect). The electric field accelerates particles in polarization direction, the magnetic field deflects them in perpendicular direction. The Stern-Gerlach force separates spin-up from spin-down fermions.

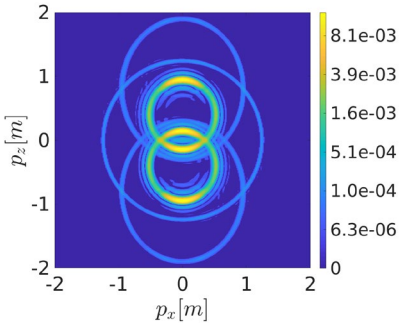

Fig.3: Momentum spectrum of electrons and positrons produced in vacuum by a standing wave pattern. Due to high-frequency modes of the background field photon-photon scattering leads to electron-positron pair production (Breit-Wheeler effect).

Gauge-Invariant Wigner Particle Model for Linear Electromagnetic Fields

M. Ballicchia, M. Nedjalkov, and J. Weinbub

Institute for Microelectronics, TU Wien

ballicchia@iue.tuwien.ac.at

Available quantum transport equations accounting for electromagnetic (EM) fields and formulated in terms of EM potentials depend on the choice of the gauge [1], [2], [3], [4]. Consequently, this requires gauge-specific solution approaches which limit physical intuition as potentials are pure mathematical quantities. We have previously suggested a Wigner equation which is formulated in terms of phase space, a quasi-distribution function, and EM forces. The equation offers a basis for developing a physically intuitive picture of a general EM fields aware quantum evolution [5]. Simplifying assumptions about the linearity of the EM fields allow to reduce the complexity of the equation [6] in favor of deeper physical insights. In this work, we associate a picture of quantum particles governed by the Lorentz force to the equation and discuss some of their properties. The physical setup corresponds to a 2D transport problem in the $\boldsymbol{x} = (x, y)$ plane and electromagnetic fields with linear spatial dependence: The magnetic field $\boldsymbol{B} = (0, 0, B(y))$ is normal to the plane and linear along y: $B(y) = B_0 + B_{1y}$. The in-plane electric field $\boldsymbol{E}(\boldsymbol{x})$ which is also assumed linear is defined as $\boldsymbol{E}(x, y) = (E_x x, E_y y)$. Under these assumptions and in the case of infinite coherence length the Wigner equation takes a very informative form

$$\left(\frac{\partial}{\partial t} + \frac{\boldsymbol{P}}{m} \cdot \frac{\partial}{\partial \boldsymbol{x}} + \boldsymbol{F}(\boldsymbol{P}, \boldsymbol{x}) \cdot \frac{\partial}{\partial \boldsymbol{P}}\right) f_w(\boldsymbol{P}, \boldsymbol{x}) =$$

$$\frac{B_1 \hbar^2}{m} \frac{e}{12} \left(\frac{\partial^2}{\partial P_y^2} \frac{\partial}{\partial x} - \frac{\partial}{\partial P_x} \frac{\partial}{\partial P_y} \frac{\partial}{\partial y}\right) f_w(\boldsymbol{P}, \boldsymbol{x}), \qquad (1)$$

where $\boldsymbol{F}(\boldsymbol{P}, \boldsymbol{x}) = e\left(\boldsymbol{E}(\boldsymbol{x}) + \frac{\boldsymbol{P} \times B(y)}{m}\right)$ is the Lorentz force and $\boldsymbol{P}$ is the kinetic momentum. The left-hand side of (1) represents the Liouville operator, which determines the classical electron evolution as in the Boltzmann equation.

However, on the right-hand side the collision operator acting on the distribution function is now replaced by an operator depending on the linear coefficient of the magnetic field B_1. If the latter becomes zero the equation consistently describes particle evolution over Newtonian trajectories. The right-hand side of the equation is thus responsible for all quantum effects. This analogy suggests to develop a particle model for the equation, which will further describe quantum effects in classical terms. Stochastic article models for the Boltzmann and the common Wigner equation (formulated in terms of the Wigner potential) are formally derived from the Fredholm integral expressions of the corresponding equations [7] which are of the form:

$$f(Q) = \int K(Q, Q') f(Q') dQ' + f_0(Q) \qquad (2)$$

However, the right-hand side of (1) contains higher-order derivatives which hinder a direct derivation of the desired integral form. We thus suggest an approximate approach: The idea is to apply a finite difference scheme to the higher-order derivatives of the right-hand side of (1). The first-order derivatives can be approximated by $\frac{\delta_{\Delta \mathrm{x}} f_w}{\Delta x}$ and $\frac{\delta_{\Delta \mathrm{P_x}} f_w}{\Delta \mathrm{P_x}}$, where

$$\begin{aligned} &\delta_{\Delta \mathrm{x}} f_w(\boldsymbol{P}, \boldsymbol{x}) = \\ &= f_w\left(\cdot, x + \frac{\Delta x}{2}, \cdot\right) - f_w\left(\cdot, x - \frac{\Delta x}{2}, \cdot,\right), \\ &\delta_{\Delta \mathrm{P_x}} f_w(\boldsymbol{P}, \boldsymbol{x}) = \\ &= f_w\left(P_x + \frac{\Delta P_x}{2}, \cdot, \cdot\right) - f_w\left(P_x - \frac{\Delta P_x}{2}, \cdot, \cdot\right). \end{aligned} \qquad (3)$$

This substitution replaces partial derivatives with shifted (position and momentum) Wigner functions. Higher-order derivatives are replaced by using corresponding finite difference schemes and are indicated by $\delta^n_{\Delta \mathrm{x}}$ and $\delta^n_{\Delta \mathrm{P_x}}$ for derivatives of order n. We use the characteristics of the Liouville operator, the Newtonian trajectories:

$$x(t') = x - \int_{t'}^{t} \frac{\boldsymbol{p}(\tau)}{m} d\tau, \boldsymbol{p}(t') = \boldsymbol{P} - \int_{t'}^{t} \boldsymbol{F}\big(x(\tau), \boldsymbol{p}(\tau)\big) d\tau \quad (4)$$

The trajectory is initialized by the point $\boldsymbol{P}$, $\boldsymbol{x}$, t, while $t' < t$ is the running time. The left-hand side of (1) becomes a full time derivative over the characteristics (4). Thus, we replace $\boldsymbol{x}$ and $\boldsymbol{P}$ in (1) by $\boldsymbol{x}(t'), \boldsymbol{p}(t')$ from (4). In particular the partial derivative $\frac{\partial f_w}{\partial x} \approx \frac{\delta_{\Delta x} f_w}{\Delta x}(\boldsymbol{p}(t'), \boldsymbol{x}(t'))$ is given by

$$\frac{f_w\big(\boldsymbol{p}(t'), x_+(t'), y(t')\big)}{\Delta x} - \frac{f_w\big(\boldsymbol{p}(t'), x_-(t'), y(t')\big)}{\Delta x}$$

with $x_\pm(t') = x(t') \pm \Delta x/2$. Next, we consider the evolution of an initial condition f_0 specified at time $t' = 0$, and integrate on t' in the interval $(0, t)$:

$$f_w(\boldsymbol{P}, \boldsymbol{x}, t) = e^{-\int_0^t \gamma(\tau) d\tau} f_0\big(\boldsymbol{p}(0), \boldsymbol{x}(0)\big) + \int_0^t dt' e^{-\int_{t'}^t \gamma(\tau) d\tau} \left[\frac{B_1 \hbar^2 e}{12m} \left(\frac{\delta^2_{\Delta \mathrm{P_x}} \delta_{\Delta_x} f_w}{\Delta P_y^2 \Delta x}(\boldsymbol{p}(t'), x(t'), t') - \frac{\delta_{\Delta \mathrm{P_x}} \delta_{\Delta \mathrm{P_y}} \delta_{\Delta_y} f_w}{\Delta P_x \Delta P_y \Delta_y}(\boldsymbol{p}(t'), \boldsymbol{x}(t'), t') \right) + \gamma(t') f_w(\boldsymbol{p}(t'), \boldsymbol{x}(t'), t') \right] \quad (5)$$

At the end of the integration the right-hand side of (5) contains linear combinations of the solution f_w so that we obtain a Fredholm integral equation of a second kind that has the form of (2): Formally, the right-hand side can be augmented by integrals on position and momentum and a set of δ-functions used in the kernel to account for the offsets introduced by the finite difference scheme. The solution is given by the resolvent series, obtained by consecutive applications of the kernel on the free term $e^{-\int_0^t \gamma(\tau) d\tau} f_0$. In this way, the solution at $\boldsymbol{P}$, $\boldsymbol{x}$, t is linked to the solutions in the phase space points $(\boldsymbol{p}(t') \pm \boldsymbol{M}\Delta\boldsymbol{P}, \boldsymbol{x}(t') \pm \boldsymbol{N}\Delta\boldsymbol{x})$ at t' over the trajectory (4), where $\boldsymbol{M}$ and $\boldsymbol{N}$ are integers introduced by the finite difference scheme. These points initialize other trajectories, so that the evolution from time t' to t becomes decomposed by Newtonian trajectories: They call for a picture of particles which evolve governed by the Lorentz force in (4). The properties of these particles bear similarities with, but also differences to, Boltzmann particles and Wigner signed particles.

We use these models as a reference frame to discuss certain peculiarities of the EM particle model. The included auxiliary function γ [6], (which factors out after taking the time derivative of the equation), can be used to determine the particle flight time according to $\gamma e^{-\int \gamma d\tau}$ in analogy with the treatment of the Boltzmann and common Wigner equations: γ refers to the total out-scattering rate in the former, whereas in the latter it refers to the interaction rate with the Wigner potential. The evolution is a result of consecutive flight and scattering events. Boltzmann particles are scattered locally in position yielding novel momentum values. All particles participate evenly in the evaluation of the physical averages, i.e., have a weight of 1. In the signed particle model the scattering is interpreted as generation of particles, which is local in position and introduces novel momentum values. The weight of the particles is, however, ± 1. EM quantum particles also obey a generation scheme, as suggested by the many components of the kernel. Furthermore, these components bear a sign due to the difference scheme and so do the EM particles. However, now the symmetry of the Wigner potential is missing so that they have different absolute weights. Finally, the introduced spatial offsets Δx show that the generation is nonlocal in position. The absolute weight difference and the spatial nonlocality is a manifestation of the quantum character of (5).

ACKNOWLEDGMENT

The financial support by the Austrian Science Fund (FWF): P33609 is gratefully acknowledged.

REFERENCES

[1] B. Novakovic et al., Phys. Rev. B 84, 195419 (2011)
[2] D. K. Ferry, Transport in Semiconductor Mesoscopic Devices (Second Edition), IOP Publishing (2020)
[3] L. Bellentani et al., Phys. Rev. B 99, 245415 (2019)
[4] G. J. Iafrate et al., Phys. Rev. B 96, 144303 (2017)
[5] M. Nedjalkov et al., Phys. Rev. B 99, 014423 (2019)
[6] M. Nedjalkov et al., Phys. Rev. A 106, 052213 (2022)
[7] M. Nedjalkov et al., Stochastic Approaches to Electron Transport in Micro- and Nanostructures, Birkhäuser (2021)

Full Counting Statistics of Ultrafast Quantum Transport

Matthias Hübler, Wolfgang Belzig

Fachbereich Physik, Universität Konstanz, D-78457 Konstanz, Germany

matthias.huebler@uni-konstanz.de

Quantum transport in the presence of time-dependent drives is dominated by quantum interference and many-body effects at low temperatures. For a periodic driving, the analysis of the full counting statistics revealed the elementary events that determine the statistical properties of the charge transport [1]. As a result, the noise correlations display quantum oscillation as functions of the ratio of the voltage amplitude and the drive frequency $eV_0/\hbar\omega$ reflecting the detailed shape of the drive. However, so far only continuous wave excitations were considered, but recently transport by few-cycle light pulses were investigated [2] and the need for a statistical interpretation became eminent.

We investigate the temporal dynamics of single- or few-cycle light pulses leaving traces in the charge transfer across nanosized gaps. The fingerprints of these time-dependent voltage pulses are imprinted in the full counting statistics of a coherent mesoscopic conductor at zero temperature. In addition, we identify the elementary processes that occur in the form of electron-hole pair creations, which can be investigated by the excess noise. We study the differential noise quantum oscillations induced by a wave packet consisting of an oscillating carrier modulated by a Gaussian- or a box-shaped envelope. As expected, the differential noise exhibits an oscillatory behavior with increasing amplitude. In particular, we find clear signature of the so-called carrier-envelope phase in the peak heights and positions of these quantum oscillations. More carrier cycles under the Gaussian envelope diminish the influence of the carrier-envelope phase, while this is not true for the box pulses, probably related to the abrupt onset.

[1] M. Vanevic, Y. V. Nazarov, and W. Belzig, *Elementary Events of Electron Transfer in a Voltage-Driven Quantum Point Contact*, Phys. Rev. Lett. **99**, 225 (2007).

[2] T. Rybka, M. Ludwig, M. F. Schmalz, V. Knittel, D. Brida, and A. Leitenstorfer, *Sub-Cycle Optical Phase Control of Nanotunnelling in the Single-Electron Regime*, Nat. Photonics **10**, 667 670 (2016).

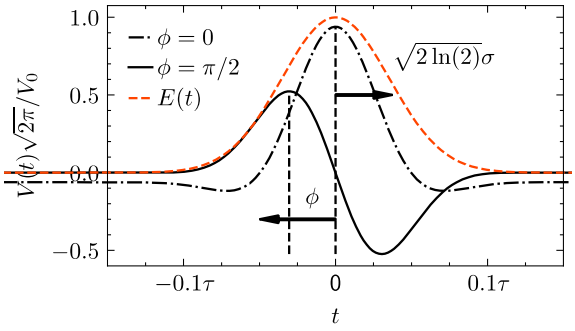

Fig.1: Gauss pulse and its envelope for carrier-envelope phases $\phi = 0, \phi = \pi/2$. The ratio between the varianceσ and the pulse repetition rate $1/\tau = \Omega/2\pi$ is chosen as $\tau/(\sqrt{2}\sigma) = 10$. Here, we set $\sigma\,\omega = 1$ (ω corresponds to the carrier frequency), which is a measure of the number of carrier cycles under the Gauss curve. Note the negative offset voltage for $\phi = 0$ to keep the average voltage at zero.

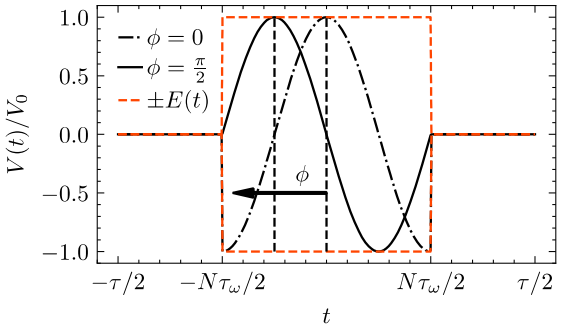

Fig.3: Illustration of the box pulse and its envelope for carrier-envelope phases $\phi = 0, \phi = \pi/2$. The box counts $N = 1$ carrier cycles with a period of $\tau_\omega$and extends between $-N\tau_\omega/2$ and $N\tau_\omega/2$, which is assumed to be smaller than the pulse repetition time τ.

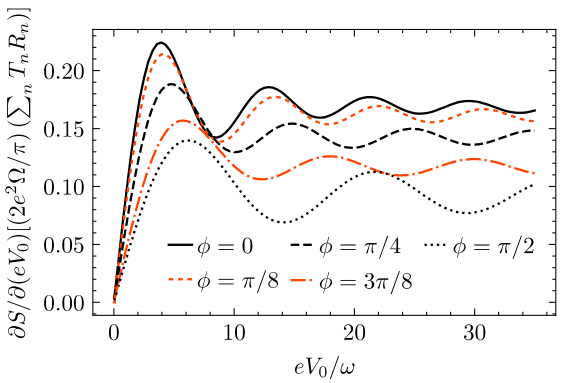

Fig.2: Differential niose $d\,S/d(eV_0)$ of a Gaussian pulse depicted over the ac amplitude V_0 for carrier-envelope phases between 0 and $\pi/2$. The variance σ in relation to the pulse repetition time τ was set to $\tau/(\sqrt{2}\sigma) = 10$ and in relation to the carrier angular frequency ω to $\sigma\,\omega = 1$.

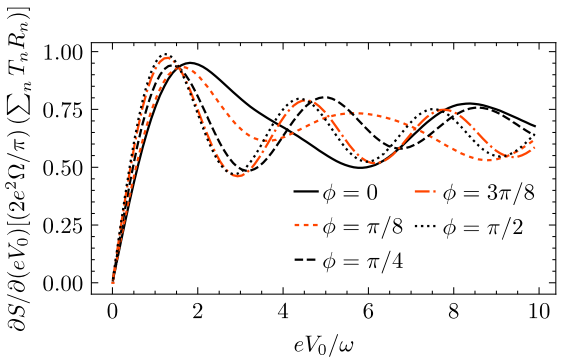

Fig.4 Differential noise $d\,S/d(eV_0)$ of a box pulse drawn over the ac amplitude V_0 for carrier-envelope phases between 0 and $\pi/2$. The number of carrier cycles is $N = 1$. The width of the box in comparison to pulse repetition rate was fixed to $\tau/(N\tau_\omega) = 2$, because the electron-hole pair creation probabilities are nearly independent of the box size. Oscillations are caused by elementary processes subsequently activated as the voltage amplitude increases.

Mitigating Phase Diffusion Through a Realistic Optical Parametric Oscillator

Stefano Olivares[1,2]

[1] *Dipartimento di Fisica "Aldo Pontremoli",*

Università degli Studi di Milano, I-20133 Milano, Italy

[2] *Istituto Nazionale di Fisica Nucleare,*

Sezione di Milano, I- 20133 Milano Italy

stefano.olivares@fisica.unimi.it

Approaches based on Wigner functions allow to deal with quantum optics problems in a clearer way, since they can better clarify the dynamics of the involved quantum states also thanks to their representation in the quantum phase-space [1]. Here we address the use of optical parametric oscillator (OPO) to counteract phase diffusion (see Fig. 1) and demonstrate phase-noise reduction for coherent signals traveling through a suitably tuned OPO [2]. In particular, exploiting the Wigner function formalism, we theoretically and experimentally show that there is a threshold value on the phase noise, above which the OPO can be exploited to "squeeze" phase noise (see Fig. 2). The threshold depends on the energy of the input coherent state, and on the relevant parameters of the OPO, i.e., gain and input-output and crystal loss rates. Applications to phase estimation in the presence of a realistic OPO are also discussed [3, 4].

[1] S. Olivares, Eur. Phys. J. Special Topics **203**, 3-24 (2012)

[2] S. Cialdi et al., Phys. Rev. Lett. **124**, 163601 (2020)

[3] G. Carrara et al., Phys. Rev. A **102**, 062610 (2020)

[4] M. N. Notarnicola et al., J. Opt. Soc. Am. **39**, 1059-1067 (2022)

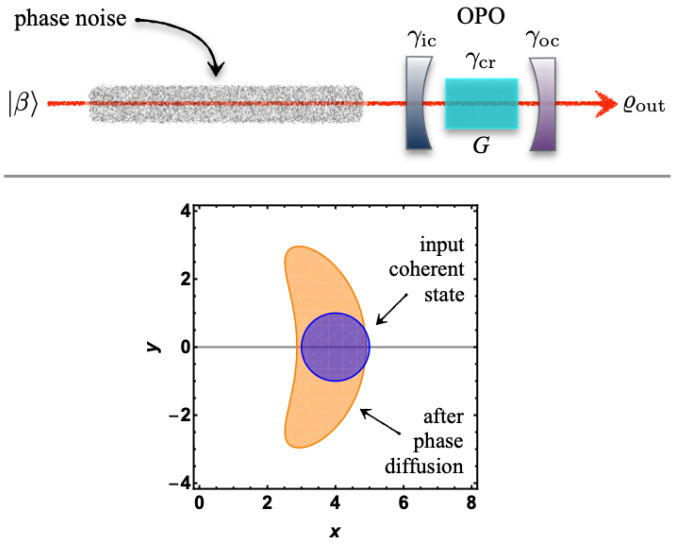

Fig.1: (Top) Experimental scheme to investigate the squeezing of phase noise. (Bottom) Phase-space representation of the Wigner function of a coherent state before (blue) and after (orange) the phase diffusion process. Picture adapted from Ref. [2].

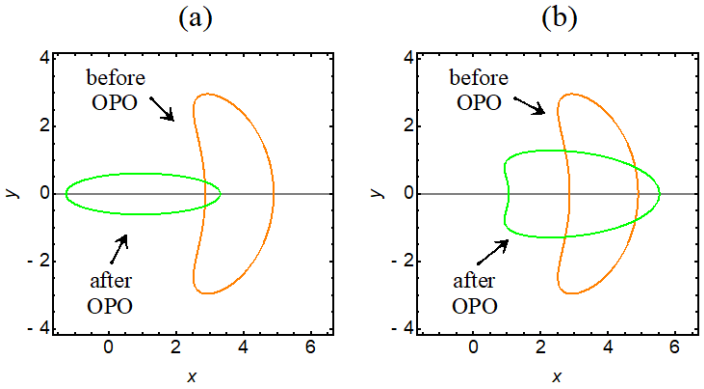

Fig.2: Phase-space representation of a coherent state after phase diffusion (orange) and after the OPO (green) for two OPO configuration (see Ref. [2] for details). Fluctuations of the y quadrature are reduced after the evolution through the OPO. Picture adapted from Ref. [2].

Wigner Approach to Optimal Control in Quantum and Classical Wave Propagation

Omar Morandi

University of Florence

Dipartimento di Matematica e Informatica U. Dini.

omar.morandi@unifi.it

I discuss some asymptotic regimes that help to clarify the connection of the Wigner-Weyl formalism with the Bohm description of the quantum mechanics and with the approximation of geometrical optics in classical highly oscillating waves. The Wigner formalism of the quasi-density distribution and the Bohm formulation of quantum mechanics provide alternative and equivalent approaches to modeling a quantum system. Both approaches describe the dynamics of a quantum particle in terms of density evolution in phase-space. Despite some formal analogies, a clear connection between the two formalisms has not been established. I will show that the Bohm description of the quantum motion can be viewed as a suitable localization limit of the Wigner pseudo-distribution function. As a second example of application of the Wigner-Weyl formalism, I will discuss the derivation of the law of optical geometry in terms of Wigner approach. I will focus on the propagation of highly oscillating field moving in inhomogeneous, dispersive media. Similarly to the classical limit in quantum mechanics, Wigner transformed high oscillating waves localize in phase-space. In the spirit of the ray propagation approximation, the wave dynamics can be approximated by a Liouville dynamical problem. Finally, I will discuss a theoretical framework in which optimal control technique can be applied to Wigner distribution function in the phase-space. The dynamics of a quantum particle is designed to steer the probability density along a path in the phase-space or to minimize some cost functional. The controlled system consists of a gas of particles in the presence of an external field and the control is achieved by a dipolar field. I will discuss the existence a solution of the optimality problem.

Functional Calculus in Phase-Space with Applications to Quantum Fluid Dynamics

Luigi Barletti

Università degli Studi di Firenze

luigi.barletti@unifi.it

We present a systematic method to compute the formal semiclassical expansion of functional calculus in the framework of the phase-space formulation of quantum mechanics. The approach is based on the holomorphic representation of functional calculus [1]. Our method allows to perform the semiclassical expansion of a large class of local equilibrium Wigner function, i.e., to express it as a leading term, corresponding to the classical distribution (Maxwell-Boltzmann, Fermi-Dirac, Bose-Einstein, etc.), plus higher-order "quantum corrections". This kind of expansion, in combination with the Quantum Maximum Entropy Principle (QMEP) [2,3], can be used to compute, starting from the Wigner equation, quantum corrections to the classical equations for fluids. This turns out to be particularly useful for systems with spin-like discrete degrees of freedom. In fact, the application of the QMEP to spinorial systems leads to peculiar difficulties (mainly related to unbounded negative energies and band singularities) that require a deep insight into the structure of the local equilibrium Wigner function [4,5].

[1] N. Dunford and J.T. Schwartz, *Linear Operators, Part I: General Theory*, Interscience, (1958)

[2] P. Degond and C. Ringhofer, J. Stat. Phys. **112**, 587-628 (2003)

[3] P. Degond, F. Méhats and C. Ringhofer, J. Stat. Phys. **118**, 625-667 (2005)

[4] L. Barletti, P. Holzinger, A. Jüngel, Kinet. Relat. Models **15**, 257-282 (2022)

[5] L. Barletti, L. Demeio and S. Nicoletti (arXiv:2211.07391)

Electrothermal Signed Particle Monte Carlo Simulation of a Resonant Tunneling Diode

Orazio Muscato

Dipartimento di Matematica e Informatica, Università di Catania, Italy

orazio.muscato@unict.it

Device self-heating is becoming one of the main technological roadblocks of the predicted device miniaturization trends. In fact, power densities are expected to reach levels that will not permit normal operation of ICs, necessitating the development of accurate electrothermal simulators to investigate new designs minimizing self-heating effects. Simulation of carrier transport in nanoscale semiconductor structures requires an accurate coupling between electronic and lattice dynamics to account for self-heating effects. Heat generation in small devices is a direct consequence of the importance of nonequilibrium carrier transport in the active region of these structures. In areas where the electric field is high, the accelerated carriers collide with the lattice resulting in the emission of a large number of phonons which contribute to heat transport in the devices. Taking advantage of previous Electrothermal Monte Carlo semiclassical models [1], we shall study the heating effect in a GaAs Resonant Tunneling Diode (RTD), coupling the Signed Particle Monte Carlo solver of the Boltzmann Wigner Transport Equation [2], [3] with a steady-state solution of the heat diffusion equation. This methodology provides an accurate microscopic description of the spatial distribution of self-heating and its effect on the detailed nonequilibrium carrier dynamics. Simulation results shell be presented during the conference.

[1] Sadi, T.; Kensal, R.W.; Pilgrim, N.; Thobel, J.L.; Dessenne, F. Monte Carlo study of self-heating in nanoscale devices. J. Comput. Electr., **11**, 118‑128, (2012).

[2] M. Nedjalkov, H. Kosina, S. Selberherr, C. Ringhofer and D. K. Ferry, Phys. Rev. B, **70**, 115319, (2004)

[3] O. Muscato, J. Comput. Electr., **20**, 2062-2069, (2021)

Interaction Time of Schrödinger Cat State with Amplitude-Varying Gaussian Potential

D. Woźniak[1], M. Kalka[1], M. Wleklińska[1], D. Kołaczek[2], M. Wołoszyn[1] , B. J. Spisak[1]

[1] *AGH University of Science and Technology, Faculty of Physics and Applied Computer Science, al. Mickiewicza 30, 30-059 Kraków, Poland*

[2] University of Agriculture in Kraków, Department of Applied Mathematics, ul. Balicka 253c, 30–198 Kraków, Poland

bjs@agh.edu.pl

The problem of tunneling time seems to be the reason for sleepless nights for many, with the main question being whether tunneling takes a finite time or simply happens instantaneously [1]. Simultaneously, the variety of tunneling time measures [2] seems unappealing, as they are based on different properties of the wave function. To unify this approach, and extend it, we suggest that the symplectic covariance of the Wigner distribution function [3] plays a significant role in determining the interaction time between quantum particles and potential. We tackle this problem by studying the interaction time of the Schrödinger cat state in a system consisting of a Gaussian potential barrier with a time-modulated amplitude with single and periodic changes. For this purpose, we applied the split operator method to solve the integro-differential equation of evolution of the Wigner distribution function and calculate the Shannon entropy and the nonclassicality parameter [4,5], two examples the of symplectically invariant measures to find the interaction times for the potential considered. Our results show that the dependence of the Shannon entropy on the trapped part of the Schrödinger cat Wigner distribution function stuck within the potential well is unnoticeable. In contrast, the corresponding nonclassicality parameter is significantly more sensitive. This results in the calculation of interaction time based on the nonclassicality parameter.

[1] A. Kheifets, J. Phys. B, **53**, 072001 (2020)

[2] E. H. Hauge, J. A. Støvneng, Rev. Mod. Phys, **61**, 917 (1989)

[3] M. de Gosson, J. Pseudo-Differ. Oper. Appl., **2**, 91 (2011)

[4] A. Kenfack, K. Życzkowski, J. Opt., B Quantum Semiclass. Opt., **6**, 396 (2004).

[5] N. C. Dias, M. de Gosson, J. N. Prata, J. Fourier Anal. Appl., **25**, 210 (2019)

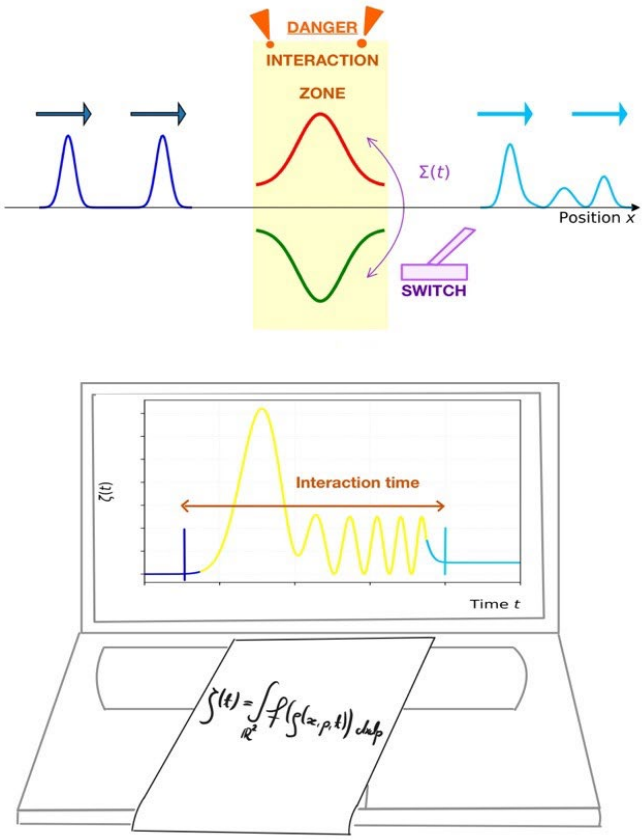

Figure 1 The visualization of the idea behind the model and the symplectically invariant measures. Yellow-marked area depicts the significant interaction zone.

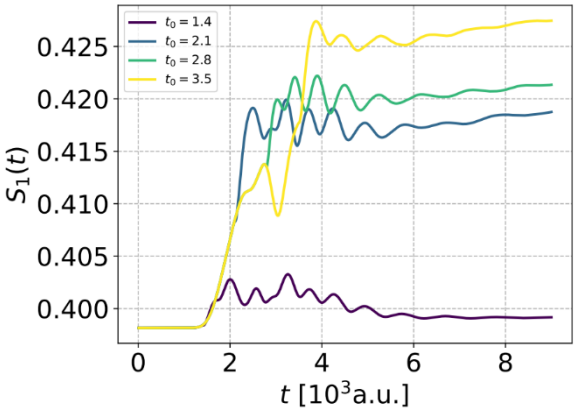

Figure 2 The implicit dependence of Shannon entropy on the time evolution of Wigner distribution function taken for different setups of switching time.

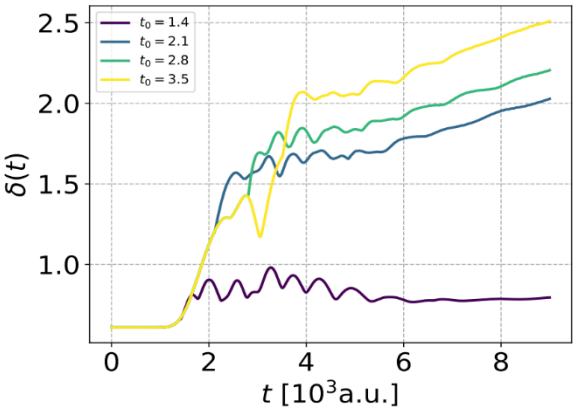

Figure 3 The implicit dependence of nonclassicality parameter on the time evolution of Wigner distribution function taken for different setups of switching time.

Scaling Laws of the Thermal Conductivity of Solids: The Role of Topological, Geometrical, and Compositional Disorder

Michele Simoncelli

Theory of Condensed Matter Group, Cavendish Laboratory, University of Cambridge (UK)

ms2855@cam.ac.uk

The temperature dependence of the thermal conductivity of crystals and glasses displays opposite asymptotic trends, decreasing as 1/T in the former and increasing (often up to a saturation value) in the latter. These trends originate from different microscopic conduction mechanisms: particle-like propagation of atomic vibrational waves in crystals [1], and wave-like tunneling between vibrational modes in glasses [2]. Recently, it has been shown that these two mechanisms naturally emerge from a unified Wigner formulation of thermal transport [3,4] (Fig. 1), raising fundamental questions on their coexistence and on related potential applications. Here we rely on such formulation to show that the relative strength of particle-like and wave-like conduction mechanisms (Fig. 2) can be regulated by varying the degree of disorder in a solid. We rely on state-of-the-art quantum-accurate computational techniques [5-8] to parametrize and solve the Wigner heat-transport equation; thus, we obtain quantitatively accurate predictions for the thermal conductivity of various families of polymorphs with variable topological (Fig. 3), geometrical, and compositional disorder. We discuss descriptors for the quantitative characterization of disorder in solids, and use them to analyze how disorder affects the magnitude and scaling law of the thermal conductivity. Finally, we show that very recent experiments confirm our prediction of the existence of materials featuring a conductivity with scaling intermediate between the 1/T decay of crystals and the increasing trend of glasses, *i.e.* almost temperature independent over a wide temperature range.

[1] Peierls, R. Ann. Phys., **395**, 1055 (1929).

[2] Allen, P. B.; Feldman, J. L., Phys. Rev. Lett., **62**, 645 (1989).

[3] Simoncelli, M.; Marzari, N.; Mauri, F., Nat. Phys., **15**, 809 (2019).

[4] Simoncelli, M.; Marzari, N.; Mauri, F., Phys. Rev. X, **12**, 041011 (2022).

[5] Erhard, L. C.; Rohrer, J.; Albe, K.; Deringer, V. L., Npj Comput. Mater., **8**, (2022).

[6] Rowe, P. et al., J. Chem. Phys, **153**, 034702 (2020).

[7] Simoncelli, M.; Mauri, F.; Marzari, N. arXiv:2209.11201 (2022).

[8] Harper, A.; Iwanowski, K.; Payne, M.; Simoncelli, M., in preparation (2023).

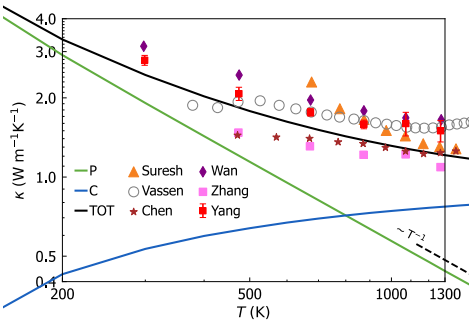

Fig. 1: Coexistence of particle-like and wave-like heat transport in $La_2Zr_2O_7$. Green, conductivity determined by particle-like conduction mechanisms (κ_P), which displays the universal T^{-1} asymptotics (dashed). Blue, conductivity determined by wave-like conduction mechanisms (κ_C). Black, total conductivity: $\kappa_{TOT}=\kappa_P+\kappa_C$ (the conductivity tensor is diagonal and isotropic). Scatter points represent the thermal conductivity measured in experiments (see Ref. [4] and references therein for details).

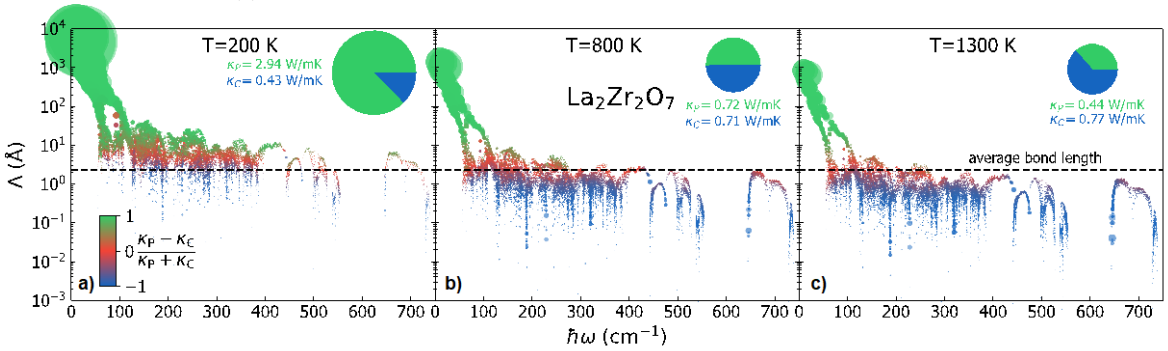

Fig 2: Phonon mean free paths as a function of energy in $La_2Zr_2O_7$ at 200 K (left), 800 K (centre) and 1300 K (right). The area of each circle is proportional to the contribution to the total conductivity and coloured according to the heat-conduction mechanism underlying the contribution: green for particle-like propagation; blue for wave-like tunneling; intermediate colours represent phonons contributing to both mechanisms, with red corresponding to 50% of each (see Ref. [4] for details). We highlight how phonons at the centre of the non-sharp crossover from dominant particle-like conduction to dominant wave-like conduction have a mean free path approximately equal to the average bond length (i.e., they are at the Ioffe-Regel limit in space, represented by the dashed line). The pie charts have an area proportional to the total conductivity, and the slices resolve the particle-like conductivity (green) and the wave-like conductivity (blue).

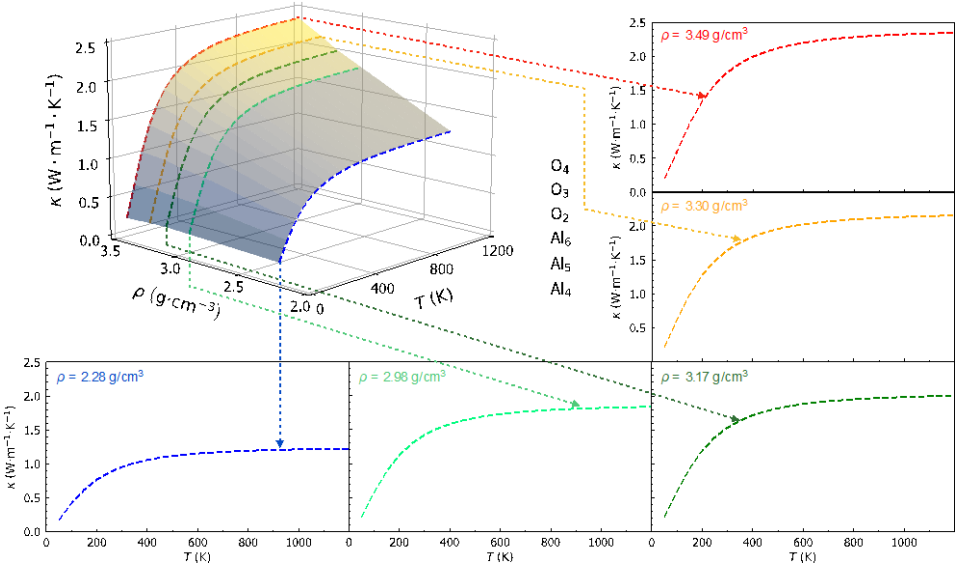

Fig. 3, Thermal conductivity of amorphous alumina with various coordination topologies. The three-dimensional plot shows the thermal conductivity determined from first principles using the regularized Wigner computational protocol discussed in Ref. [7]. The two-dimensional plots show how the coordination topology of the disordered amorphous alumina network changes with density, and how this affects the total thermal conductivity. Taken from Ref. [8].

Scattering In the Wigner Equation

S. W. Belling and I. Knezevic

Department of Electrical and Computer Engineering, University of Wisconsin – Madison

Madison, WI 53706

swbelling@wisc.edu

ABSTRACT

The Wigner equation describes the time evolution of the Wigner function, a quantum-mechanical analogue to the phase-space distribution function for a particle in classical statistical mechanics. We describe a procedure for calculating the collision integral in the Wigner equation, which would describe scattering in quantum-transport applications of the Wigner equation. We start from expressions for the dissipator term in the density matrix approach and project the terms onto a continuous momentum basis, where the Wigner-Weyl transform that moves us from the density matrix to the Wigner equation gets simplified.

INTRODUCTION

There are three popular quantum transport formalisms, each with their own benefits and drawbacks. The density matrix approach can capture full time-evolution in a computationally efficient manner, but relies on gauge-dependent formulations of electromagnetic fields which can be complicated to obtain. The non-equilibrium Green's function (NEGF) approach deals well with scattering, but is generally limited to steady-state problems due to computational cost [1]. The Wigner function can capture full time-evolution like the density matrix, and is also expressed in terms of a familiar phase-space (coordinate and momentum), which makes comparisons to classical physics intuitive [1]. However, the question remains open of how to treat scattering in a detailed microscopic way that is numerically tractable and intuitively appealing. Here, we present our steps toward tackling this treatment of scattering.

APPROACH

The Wigner function evolves in time according to the Wigner equation (1) which in 1D can be written as

$$\frac{\partial f_W}{\partial t} + \frac{p}{m^*}\frac{\partial f_W}{\partial x} = Q f_w(x,p) + C[f_w(x,p)] \qquad (1)$$

where f_W is the Wigner function, V_W is the so-called Wigner potential, x is the coordinate and p is momentum. The right hand side of this equation includes all scattering terms in the collision operator $C[f_w(x,p)]$. To obtain these scattering terms, we first look at the equation of motion for the density matrix, written in the Schrödinger picture as [2]:

$$\frac{d\rho_e}{dt} = -\frac{i}{\hbar}[H_0, \rho_e(t)] - \frac{1}{\hbar^2}\int_0^\infty tr_{ph}\{[H_I, [\boldsymbol{H_I}(\tau), \rho_e(\tau) \otimes \rho_{ph}(0)]]\}d\tau, \quad (2)$$

where the important quantity is H_I, the interaction Hamiltonian, which we can write for each scattering mechanism. The result of the time integral in (2) using a common bath spectral function is shown in Fig. 2. Typically, H_I is cast in a basis of discrete energy eigenstates, where the rotating-wave approximation (RWA) is used to simplify the calculations. The RWA relies on the assumption of discrete energy states and large energy level spacings, which is not accurate for open or periodic systems, as in Fig. 1. Instead, we project H_I onto the continuous momentum basis, making each term more suitable to be Wigner-Weyl transformed into the Wigner formalism. For example, one scattering mechanism might have an interaction Hamiltonian of the form

$$\left(\frac{2\pi}{L}\right)^2 \iint dk dk' M(k,k') E(q) C_{k'}^+ C_k \otimes B(\tau), \quad (3)$$

where $M(k,k')$ is the matrix element connecting states k, k' and $C_k, C_{k'}^+$ are electronic creation and destruction operators, and B (for bath) is an operator for the other interacting particle (phonon, photon, etc.). Finally, we transform (3) to the Wigner equation with the Wigner-Weyl transform, aided by our projection to momentum which is already one of the Wigner function parameters.

ACKNOWLEDGMENT

The authors gratefully acknowledge support from the US Department of Energy, Basic Energy Sciences, Award DE-SC0023178.

REFERENCES

[1] J. Weinbub and D. K. Ferry, *Recent advances in Wigner function approaches*, Appl. Phys. Rev. **05**, 041104 (2018).

[2] F. Karimi, A. H. Davoody, and I. Knezevic, *Dielectric function and plasmons in graphene: A self-consistent-field calculation within a Markovian master equation formalism*, Phys. Rev. B **93**, 205421 (2016).

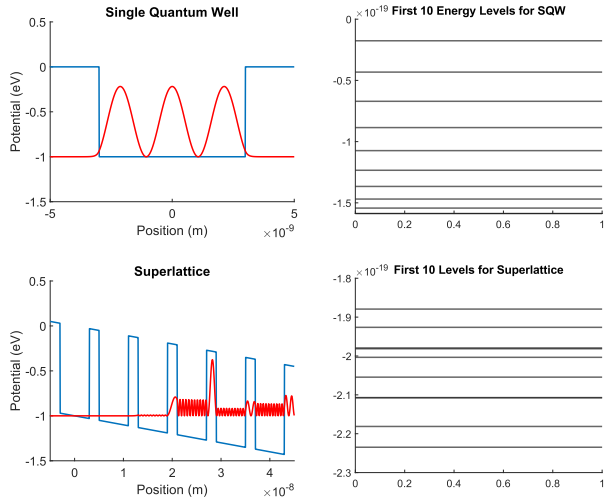

Fig. 1. Comparison of energy level spacings for a single quantum well (top) and several quantum wells (superlattice) (bottom). Even with just a few quantum wells stacked together, some of the energies begin to cluster together, decreasing the validity of the RWA. In a periodic structure or a true open system, the energy spectrum is continuous and the RWA unusable.

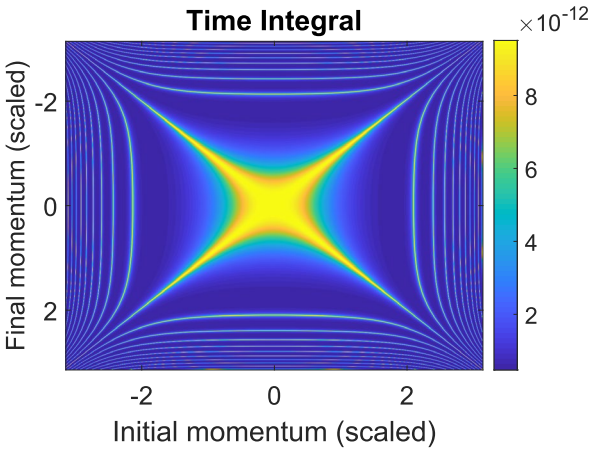

Fig. 2. Calculation of the time integral on the RHS of equation (2) for a simple representative elastic scattering mechanism in a periodic system.

Real-Space Treatment of Polar-Optical Phonons with Wigner Functions

David K. Ferry

School of Electrical, Computer, and Energy Engineering, Arizona State University,

Tempe, AZ 85287-5706 USA

ferry@asu.edu

It is generally difficult to treat long-range Coulombic scattering with perturbation theory, if for no other reason than the very common existence of multiple scattering. This is especially true with impurity scattering [1], and the coherence that exists through the scattering has been shown to be important in quantum transport [2]. In treating the polar-optical phonon interaction with non-equilibrium Green's functions, one has to worry about these correlations, which may lead to the need to include solving the Bethe-Salpeter equation and consideration of disconnected diagrams. A more useful approach is to use Wigner functions, as it has already been demonstrated that Monte Carlo techniques may be used here. The complication is the determination of the Wigner potential arising from the dipole interactions (fig. 1, 2) of the polar-optical phonon in real space that has been proposed [3]. Here, the determination of this Wigner potential and the constraints that Wigner transport faces when simulating the polar modes in real space will be discussed, using a planar semiconductor device configuration in which transport, and the Wigner function, are treated in the longitudinal (transport) direction of the channel, which is oriented along (110). In this configuration, the dipole fields are oriented at an angle to the plane of the channel (fig. 3), with this angle determined by crystalline properties. The projection of the dipole potential onto the channel plane maintains a dipolar potential, in which the amplitude is varied by the projection angle. The transformation of this potential into the Wigner potential is discussed, maintaining the three-dimensional nature of the original dipoles. The temporal modulation of the potential due to the phonon frequency sets a time scale which must be utilized in the simulations, if the scattering is to be observed.

[1] H. S. Wong and Y. Taur, IEDM (1993) p.705.

[2] J. Weinbub *et al*., Phys. Stat. Sol. RRL **12**, 1800111 (2018).

[3] D. K. Ferry, IWCN 2023

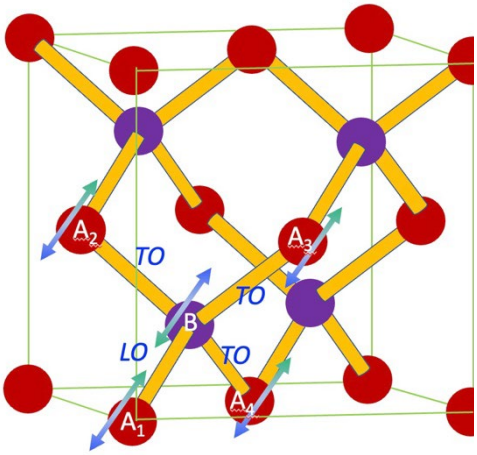

Fig. **2**. Motion of the atoms on one basis set may be the LO mode, simultaneously the other atoms in the tetragonal bonding are undergoing TO motion.

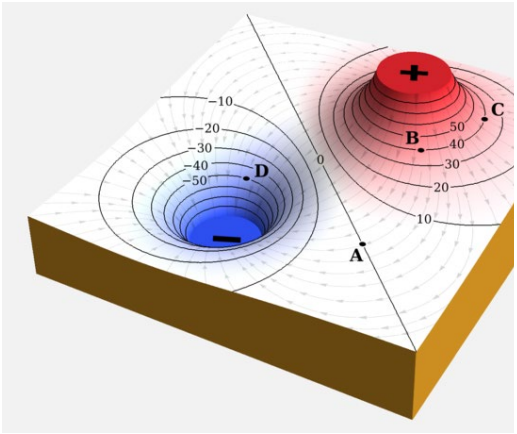

Fig. 2. A dipole potential. The dipole charge is aligned along the (111) crystal axis. (Wikipedia Commons 3.0)

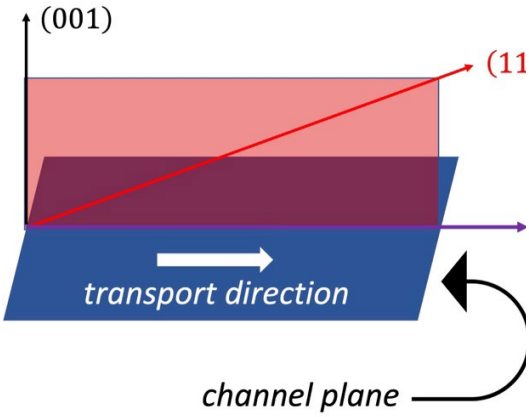

Fig. 3 Orientation of the channel plane and the direction of the actual dipoles (111).

Minimum Uncertainty States with Wigner: Quantum Hydro-Thermodynamics

Nezihe Uzun

Center for Theoretical Physics, Polish Academy of Sciences, Warsaw, Poland

nuzun@cft.edu.pl

This talk is based on our previous work [1] whose main aim is to explore certain connections between classical and quantum systems in phase space. As the minimum uncertainty states are the closest one can get to a classical picture, squeezed coherent states are the main actors of this investigation. Those are time–dependent, Gaussian states and their Wigner functions are also known to be Gaussian. This allows one to treat the Wigner function of squeezed coherent states as a well–defined quantum phase space distribution. We show that once one considers the hydrodynamic interpretation of quantum mechanics in tandem with the Wigner–Weyl–Moyal approach, a dynamic equilibrium thermodynamics of the system is derived quite easily similar to the one in classical kinetic theory.

Within this talk, we show that (i) the Wigner function can be used to identify a marginal position distribution and a conditional momentum distribution together with their corresponding equilibrium entropies, (ii) temperature, pressure and internal energy can be derived for a dynamic quantum system; their connection to the quantum potential, the Maslov index and virial relation can be identified, (iii) different elements of the classical symplectic phase space evolution guide the evolution of different parts of the quantum thermodynamical potentials.

We believe those results might find some area of use within the quantum information and quantum engineering applications. Specifically in quantum opto–mechanical problems where stability and efficiency issues are open problems for time dependent systems.

[1] N. Uzun, Annals of Physics, Vol. 442, 168900 (2022).

Overcoming the Numerical Sign Problem in the Wigner Dynamics via Adaptive Particle Annihilation

Yunfeng Xiong

Beijing Normal University

yfxiong@bnu.edu.cn

The infamous numerical sign problem poses a fundamental obstacle to particle-based stochastic Wigner simulations in high dimensional phase space. Although the existing particle annihilation via uniform mesh significantly alleviates the sign problem when dimensionality $D \leq 4$, the mesh size grows dramatically when $D \geqslant 6$ due to the curse of dimensionality and consequently makes the annihilation very inefficient.

In this talk, I would like to report our recent progresses in overcoming the sign problem, based on a series of joint work with Professor Sihong Shao at Peking University, China. The first is a variance reduction technique based on the stationary phase approximation to kill the redundant stochastic particles. The second is an adaptive particle annihilation algorithm, termed Sequential-clustering Particle Annihilation via Discrepancy Estimation (SPADE). Specifically, SPADE follows a divide-and-conquer strategy: Adaptive clustering of particles via controlling their number-theoretic discrepancies and independent random matching in each cluster. The target is to alleviate the oversampling problem induced by the over-partitioning of phase space and capture the non-classicality of the Wigner function simultaneously. Combining them together, we attempt to simulate the proton-electron couplings in 6-D and 12-D phase space. A thorough performance benchmark of SPADE is provided with the reference solutions in 6-D phase space produced by a massively parallel grid-based deterministic Wigner solver.

[1] Y. Xiong and S. Shao, Overcoming the numerical sign problem in Wigner dynamics via particle annihilation, http://arxiv.org/abs/2008.05161.

[2] Y. Xiong and Y. Zhang and S. Shao, A characteristic-spectral-mixed scheme for six-dimensional Wigner-Coulomb dynamics, https://arxiv.org/abs/2205.02380.

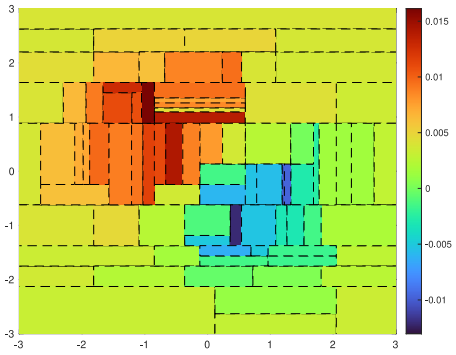

Fig.1: Adaptive clustering of positive and negative particles

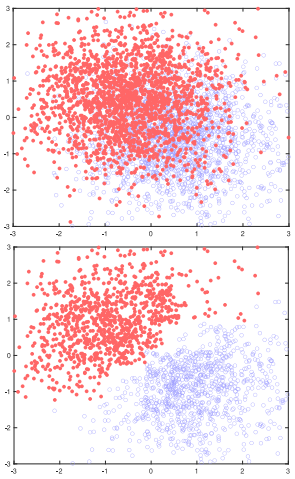

Fig.2: Particles before and after adaptive annihilation

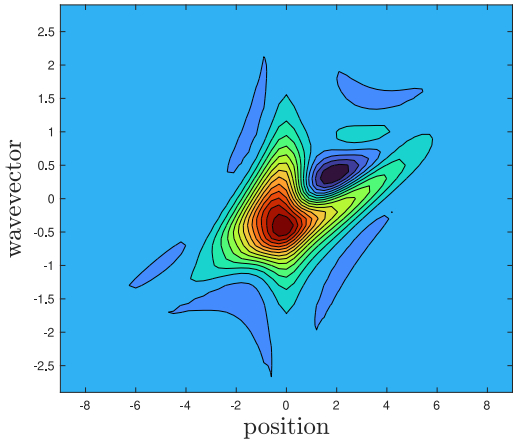

Fig.3: Deterministic solutions of the Wigner function under the Coulomb potential.

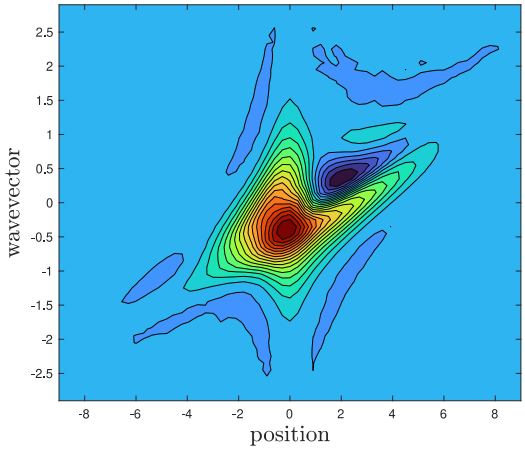

Fig.4 Stochastic particle solutions of the Wigner functions after SPADE.

Towards the Intuitive Understanding of Quantum World: Sonification of Wigner Function

Reiko Yamada[1], Eloy Pinol Jimenez[1], and Maciej Lewenstein[1,2]

[1] *ICFO-Institut de Ciencies Fotoniques, The Barcelona Institute of Science and Technology*

08860 Castelldefels (Barcelona), Spain

[2] *ICREA, 08010 Barcelona, Spain*

reiko.yamada@icfo.eu

epinol@icfo.net

In recent years, there has been a resurgence of interest in quantum technologies by the general public. However, there has not been a convincing explanation of what exactly quantum mechanics is and how does the quantum world differ from the classical, formulated in a language that the public can comprehend. The problem of understanding quantum phenomena lies on the fact that they substantially differ from our perception of the everyday classical world alongside its intuitive interpretation. The visualization of the Wigner function, for example, has been widely used to develop the link between the two worlds, however the outcome at present is far from being ideal. Instead, our team, comprising a composer and quantum physicists, experimented with sonification in order to hone out intuition when coming across quantum phenomena. For this purpose, we focus on two characteristic examples, the n-photon (Fock) states and a "cat" state formed as a superposition of two coherent states resulting from a high-harmonic generation process. The latter is the highest photon number optical "cat" state experimentally reported [1], and varying the shift of the superposition it goes from a cat to an almost coherent state. Then, we sonify a transition from a quantum to an almost classical state. This paper illustrates a couple of methods we employed when experimenting with the Wigner-function sonification. The first one entails a mapping of its values to amplitudes, frequencies and phases of waveforms, superimposed to produce the final outcome. The second one maps the volume of different segments to the intensity of the desired sound outcome, while the extrema attained in each segment correspond to musical intervals in the score to be distributed to string quartet.

[1] J. Rivera-Dean et al, Phys. Rev. A 105, 033714 (2022)

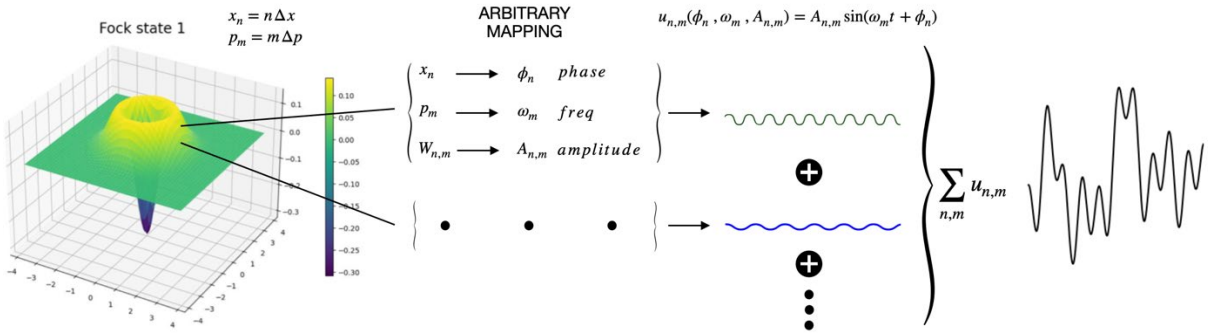

Fig.1: Fock state 1 and an example of mapping to sound. Each point of the grid is mapped to a waveform. Summing over them yields the final soundwave.

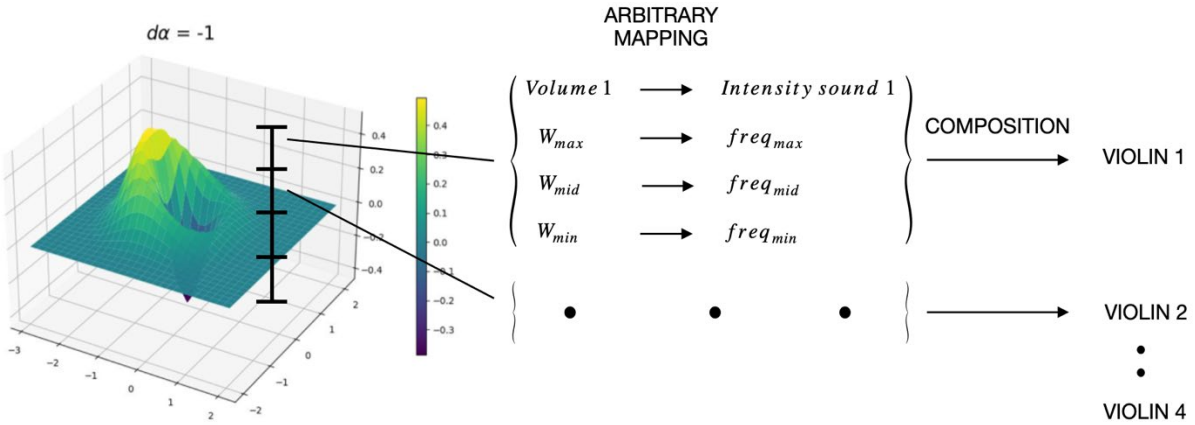

Fig.2: Cat state with shift δα= -1 setting another example of mapping to sound.

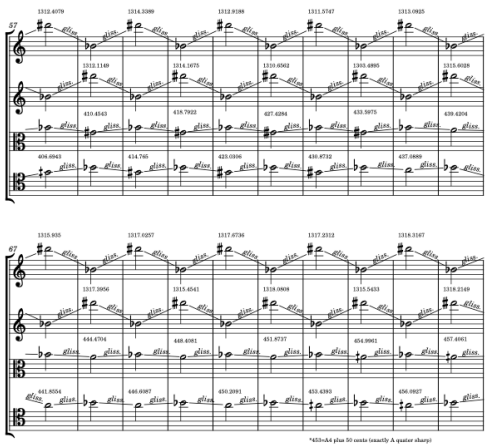

Fig.3: Score example of Wigner Function representation in String Quartet.

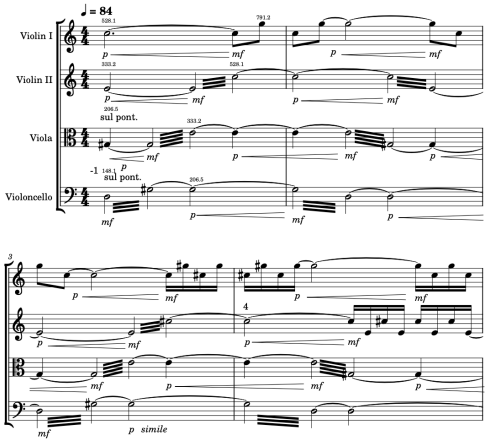

Fig.4: Score example of Wigner Function representation in String Quartet.

Investigation of a Staggered Grid Formulation of the Wigner Transport Equation for Complex Band Structures

Mathias Pech, Alan Abdi and Dirk Schulz

Chair for High Frequency Techniques, TU Dortmund, Germany

mathias.pech@tu-dortmund.de

Describing the quantum charge carrier transport within the Wigner formalism offers many advantages including ease of transient simulations, low computational effort and the ability to include scattering. However, one problem common to all related approaches arises from the inherent transformation onto center-of-mass coordinates: Half of the density matrix is essentially lost when using a uniform grid [1]. Previous attempts at including the missing grid points resulted in a staggered grid formulation for the Wigner transport equation but suffered from their own drawbacks, such as the need for artificial scattering terms and the occurrence of negative charge carrier densities ([2]). With the presented approach, a similar formulation of two staggered grids occurs naturally when trying to model complex band structures, but the flexibility of a possible extension to non-parabolic bands is retained. An additional benefit is the similarity to the tight binding method, with the two approaches being equal in case of parabolic bands, which correspond to a next-nearest neighbor approximation. Meanwhile, the conventional finite volume Wigner approach is inherently included when the potential is approximated by middle point rule, essentially decoupling the two grids. In order to approximate the energy dispersion in semiconductors, two common approaches are the power series expansion or the decomposition into its Fourier components. The former approach results in many derivative terms after the inverse-Weyl transformation that need to be approximated. The latter approach, however, results in exponential functions that directly lead to a discretization scheme similar to a central finite difference scheme and no derivatives need to be approximated. Two staggered grids result, which are coupled via the potential and pose novel challenges regarding their boundary conditions and reflections in the finite computational domain. The latter can be dealt with by using a complex absorbing potential (CAP) [3], that has to be modified for the formalism. The formulation of inflow boundary conditions proves to be difficult, since one of the grids always lies nested within the device and not at the contacts. The presented approach shows promising results and should therefore be further investigated for energy bands beyond the parabolic approximation and different boundary conditions.

[1] W.R. Frensley, Rev. of Mod. Phys., **62**, 745 (1990)

[2] R.K. Mains, G.I. Haddad, J. Comput. Phys., **112**, 149 (1994).

[3] L. Schulz, D. Schulz, Trans. Nanotechnol. **18**, 830 (2019)

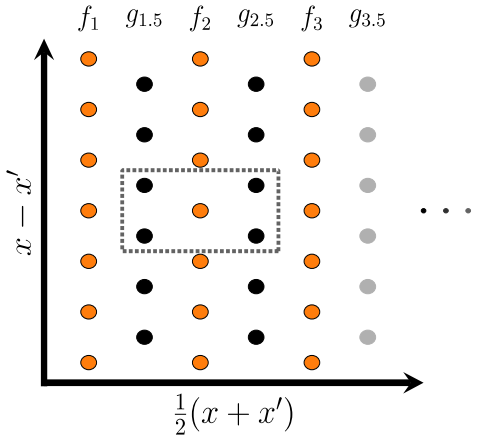

Fig.1: The staggered grid in real space consists of the subgrids f and g as a result of the transformation onto the center-of-mass coordinates. For parabolic bands the potential couples the adjacent grids to each other. The dashed box indicates the computational cell for the centermost point in f_2. When higher order approximations are used, the computational cell is extended to further grid points, similar to a higher order finite difference scheme. Special care has to be put into the inflow boundary conditions for f and g, as the first and last slices of g lie within the device and not at the boundary to the infinite reservoir.

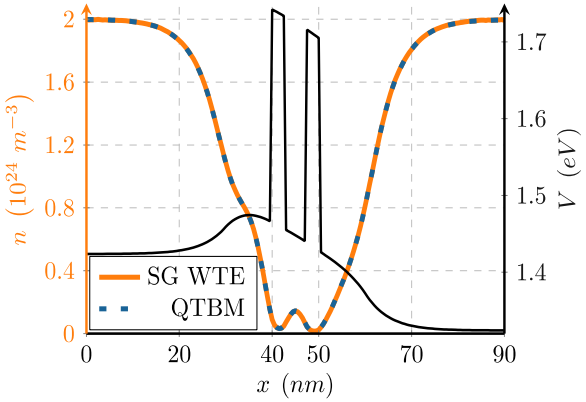

Fig.3: The self-consistent potential U and charge carrier density n as obtained by the presented algorithm (SG WTE) are shown for a resonant tunneling diode (RTD) when a drain voltage of 0.1 V is applied. The charge carrier density converges only when an appropriate CAP [3] is utilized. Similarly, the current densities are strongly influenced by the choice of the CAP and quickly diverge to unphysical results when unsuitable parameters for the CAP are chosen. As it can be seen the results are in excellent agreement with reference results obtained with the QTBM (dashed).

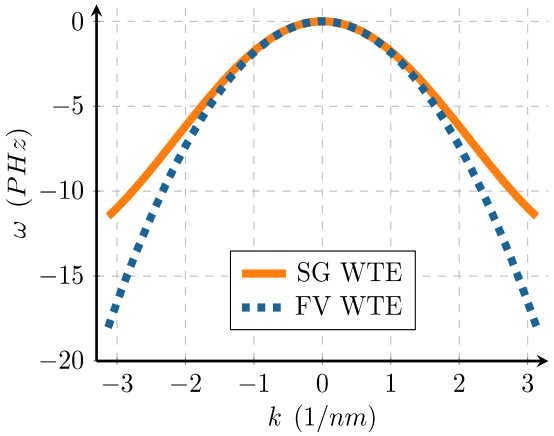

Fig.2: Numerical dispersion for the presented approach using staggered grids (SG WTE) and for a standard finite volume discretization of the Wigner Transport equation (FV WTE). The solid line shows the dispersion for the case of parabolic bands as it is considered here. An extension to more complex bands is natural to the formalism and should be investigated further.

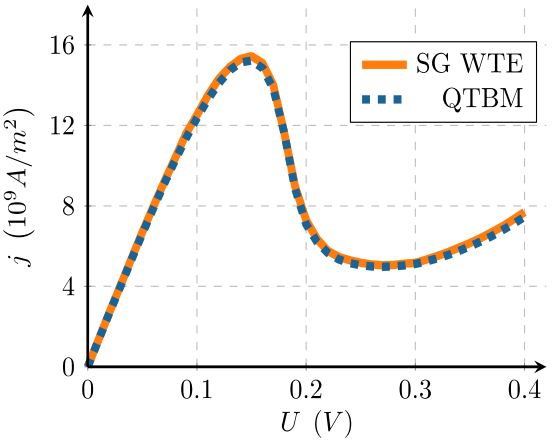

Fig.4: The drain-end current density of the staggered grid approach is in excellent agreement to a reference solution obtained with the QTBM. For the staggered grid the arithmetic mean of the drain-end current densities of both grids is shown. Even though the individual current densities diverge from each other for higher drain voltages the mean current density is still smooth. In order for the self-consistent Gummel algorithm to converge at higher applied voltages, the contacts of the RTD have been lengthened and the permittivity of the device has been artificially increased towards the contacts. This indicates that further investigation towards appropriate boundary conditions is needed.

Operational Phase-Space Distribution Functions Through Consecutive Weak and Strong Measurements

Xavier Oriols and Carlos F. Destefani

Departament d'Enginyeria Electrònica, Universitat Autònoma de Barcelona

08193, Bellaterra, Barcelona, Spain

The Wigner distribution $\boldsymbol{f_W}(x,p,t)$ is a phase-space function that provides the correct (position and momentum) marginal distributions. In particular, it can be used to compute the weak values of the momentum in a (post-selected) position $p_W(x,t)$, also known as Bohmian velocities [1]. However, such Wigner distribution function can have negative values in some points or regions of the phase-space so that, strictly speaking, it cannot be understood as a probability, but as a quasi-probability [2]. Alternatively, in the laboratory, the weak value of the momentum $p_W(x,t)$ can be obtained from the expression $p_W(x,t) = \int dp\ p\ \boldsymbol{P_{px}}(p,x,t)\ / \int dp\ \boldsymbol{P_{px}}(p,x,t)$, where the probability distribution $\boldsymbol{P_{px}}(p,x,t)$ is constructed from the following operational protocol using an ensemble of identically prepared quantum states: (i) for each initial state of the ensemble, first, a weak measurement of the momentum is done, yielding the value p at time t; (ii) subsequently, a strong measurement of the position is done, yielding the value x at time t. Finally, $\boldsymbol{P_{px}}(p,x,t)$ is constructed by counting how many p and x occur when repeating (i) and (ii) on the mentioned ensemble [3]. By construction, $\boldsymbol{P_{px}}(p,x,t)$ is always positive so that it is a true probability distribution in phase-space. In a similar way, one can construct $\boldsymbol{P_{xp}}(p,x,t)$ when first measuring the position weakly and after the momentum strongly. Again, by construction, $\boldsymbol{P_{xp}}(p,x,t)$ is also a true probability distribution in phase-space. In this workshop, we will study which are the similitudes and differences between the Wigner function $\boldsymbol{f_W}(x,p,t)$ and the new operational phase-space functions $\boldsymbol{P_{px}}(p,x,t)$ and $\boldsymbol{P_{xp}}(p,x,t)$ plotted in Figs 1, 2 and 3, respectively, for the superpositions of the gaussian states described in Fig. 1. Figure 4 shows that $\boldsymbol{P_{px}}(p,x,t)$ provides the correct marginal distributions when integrated along the momentum, while the marginal distributions integrated in position are not correct because their still depend on the ancilla wave packet. In a similar way, Fig. 5 shows that $\boldsymbol{P_{xp}}(p,x,t)$ provide the correct marginal distributions when the integrated along the position, while the marginal distribution integrated along momentum is incorrect. In Fig. 6, we see that the Bohmian velocity (in the mentioned above expression) can be equivalently computed from $\boldsymbol{f_W}(x,p,t)$ or $\boldsymbol{P_{px}}(p,x,t)$. We argue that these two phase-space functions $\boldsymbol{P_{px}}(p,x,t)$ and $\boldsymbol{P_{xp}}(p,x,t)$ contain the same information that can be extracted from $\boldsymbol{f_W}(x,p,t)$ with the advantages that they are positive-defined, have a simple and natural (no interferences in the phase-space central region) interpretation and are easily accessible in the laboratory through weak measurements. We conclude that such phase-space functions $\boldsymbol{P_{px}}(p,x,t)$ and $\boldsymbol{P_{xp}}(p,x,t)$ clearly merit further investigation.

[1] D.Pandey, R.Sampaio, T.Ala-Nissila, G. Albareda, and X. Oriols; Phys. Rev. A, 103, 052219 (2021).

[2] E. Colomes, Z. Zhan, X. Oriols Journal of Computational Electronics, 14, 894(2015)

[3] Carlos F. Destefani and Xavier Oriols, Phys. Rev. A 107, 012213 (2023).

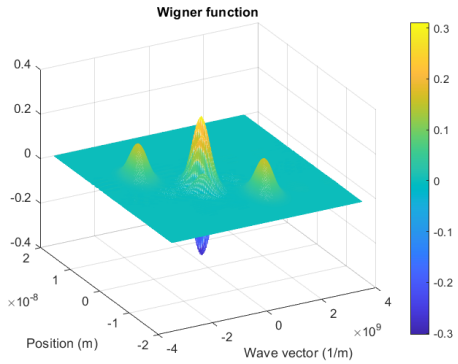

Fig. 1: Wigner distribution function $\boldsymbol{f_W}(x,p,t)$ for a superposition of two wave packets. One with central position -10 nm and momentum 2 nm^{-1} and another with central position 5 nm and central momentum -1 nm^{-1}. Both with spatial dispersion of 4 nm. Such superpositions provide negatives (quasi)probabilities. See interference in the phase-space central region.

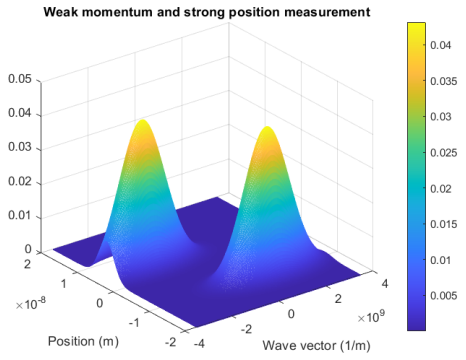

Fig. 2: Operational phase-space distribution function $\boldsymbol{P_{px}}(p,x,t)$ obtained in a laboratory from a weak momentum measurement (with and ancilla wave packet with dispersion $\sigma_k = 1.75\ nm^{-1}$) and a consecutive strong position measurement for the quantum state described in Fig 1. No negative probabilities and no interferences in the phase-space central region.

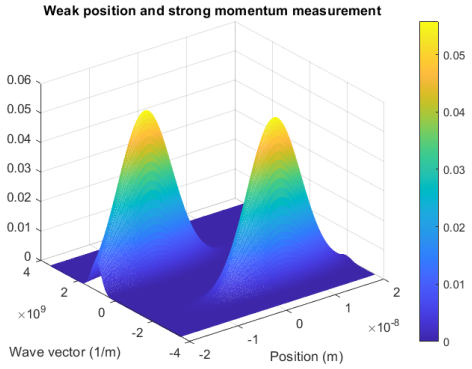

Fig. 3: Operational phase-space distribution function $\boldsymbol{P_{xp}}(p,x,t)$ obtained in a laboratory from a weak position measurement (with an ancilla wave packet with dispersion $\sigma_x = 10\ nm$) and a consecutive strong momentum measurement for the state in Fig 1. No negative probabilities and no interferences in the phase-space central region.

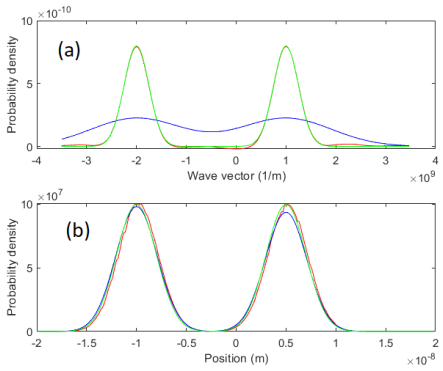

Fig. 4: Marginal probability distributions as a function of wave vector (a) and as a function of position (b) computed from the Wigner function from Fig. 1 (red) and the distribution $\boldsymbol{P_{px}}(p,x,t)$ from Fig. 2 (blue). The position and momentum distribution directly computed from the wave function are also plotted (green).

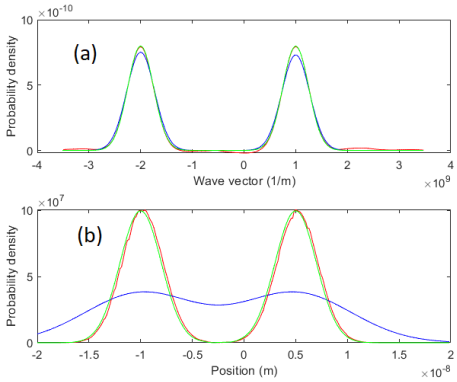

Fig. 5 Marginal probability distributions as a function of wave vector (a) and as a function of position (b) computed from the Wigner function from Fig. 1 (red) and the distribution $\boldsymbol{P_{xp}}(p,x,t)$ from Fig. 3 (blue). The position and momentum distribution directly computed from the wave function are also plotted (green).

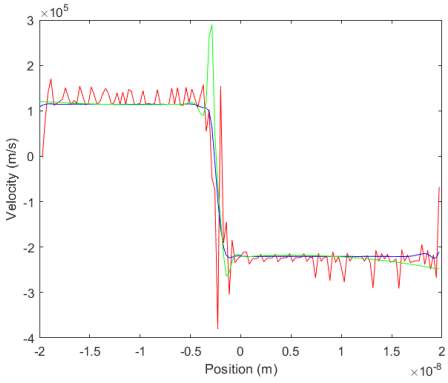

Fig. 6: Bohmian velocity computed from the wave function (green), from the Wigner distribution (red) and from the distribution $\boldsymbol{P_{px}}(p,x,t)$ (blue).

Dynamics-Based Certification of Quantumness

Lin Htoo Zaw[1], Pooja Jayachandran[1], Clive Cenxin Aw[1] and Valerio Scarani[1,2]

[1] *Centre for Quantum Technologies, National University of Singapore, Singapore*

[2] *Department of Physics, National University of Singapore, Singapore*

physv@nus.edu.sg

Inspired by a 2006 work by Tsirelson that went completely unnoticed [1], we developed a new method to certify the non-classicality of some states [2-4]. The criterion assumes the knowledge of the dynamics that the system under study is undergoing. The talk will focus on our results for uniform precessions, although we have been able to extend the criterion to several other evolutions. For continuous variables, the main features of this certifications are:

- It achieves a score that no classical model can match (like Bell's inequalities). By contrast, most criteria for quantumness and entanglement rely on the uncertainty relations and are thus vulnerable to false positives in the case of imperfect measurements or calibration.
- The protocol requires a single measurement of a single quadrature in each round. This in contrast with the Leggett-Garg criterion, that requires sequential measurements; and with criteria based on contextuality, which require defining sets of compatible observables.
- It detects non-Gaussian states; and the optimal states form a family that can be used for bosonic error correction codes.

Overall, the main surprise is: who would have said that one could detect quantumness by observing a boring uniform precession, as classical as it gets?

[1] B. Tsirelson, https://arxiv.org/abs/quant-ph/0611147

[2] L.T. Zaw et al., Phys. Rev. A 106, 032222 (2022), https://arxiv.org/abs/2204.10498

[3] P. Jayachandran et al., https://arxiv.org/abs/2210.10357

[4] L.T. Zaw, V. Scarani, https://arxiv.org/abs/2212.06017

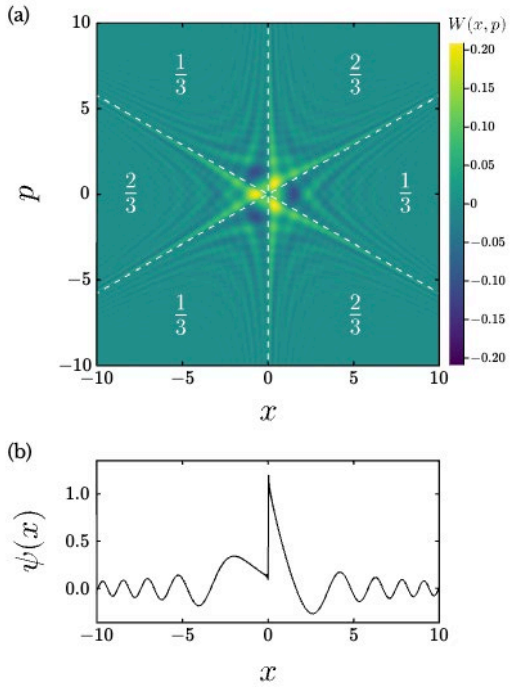

Fig.1: Wigner function and wave-function of the harmonic oscillator state that is optimally detected by our protocol with three measurement times. From [2].

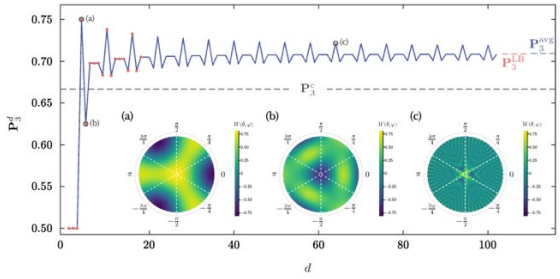

Fig.2: The criterion applied to the precession of angular momentum for discrete systems: optimal quantum score as a function of the Hilbert space dimension. In the inset, Wigner functions obtained by projecting the state on an overcomplete basis of states that encode a direction on a sphere. From [2].

Phase Space Representation of Time-Frequency as Quantum Continuous Variables: Universal Quantum Computing, Metrology and the Quantum-Classical Frontier

Pérola Milman[1], Eloi Descamps[1], Nicolas Fabre[2], Arne Keller[3]

[1] *Laboratoire Matériaux et Phénomènes Quantiques, Univ. Paris Cité, CNRS*

[2] *Télecom ParisTech*

[3] *Univ. Paris-Saclay*

perola.milman@u-paris.fr

Modes of the electromagnetic field appear both in classical and quantum optics. Nevertheless, when associated to quantum fields, as single photons, modes inherit of the photonic commutation relations and can thus be used in various applications, as testing fundamental aspects of quantum physics [1] or quantum computation and communications [2]. In such applications one often uses polarization as a discrete mode and map a qubit into orthogonal polarization states.

In the present contribution we focus on continuous modes of single photons, and study in details the case of frequency and time variables. We show that, when associated to a subspace of n single photons, these variables also reproduce the commutation relations of position and momentum, or orthogonal quadratures of the electromagnetic field. Thus, it is possible to implement, with single photons, all the existing protocols for quantum computation and communication with continuous variables. Nevertheless, doing so requires some effort in defining a classical reference in phase space and leads to a different interpretation of the Wigner function's properties than the one developed for the field's quadratures.

We construct all the necessary theoretical tools to define universal quantum gates using time and frequency as continuous variables and connect them to experimental devices that are currently used in quantum optics laboratories [3]. Then, we then study in details the role of the electromagnetic field's frequency in time precision measurements using single photons as a paradigmatic system. For such, we independently identify the contributions of intensity and spectral resources and show that both can play a role on the scaling of the precision of parameter estimation with the number of probes. We show in particular that it is possible to observe a quadratic scaling using quantum mode correlations only and explicit the mathematical expression of states saturating the Heisenberg limit. We also provide a geometrical and phase space interpretation of our results, and observe a curious quantum-to-classical-like transition on scaling by modifying the spectral variance of states. Our results connect discrete and continuous aspects of single photons and quantum optics by considering from a quantum mechanical perspective the role of frequency [4].

Finally, we propose a way to directly measured the Wigner function and the Quantum Fisher Information of a collective variable associated to a photon pair using modifications of the Hong-Ou-Mandel experiment [5,6].

[1] A. Aspect, P. Grangier, and G. Roger, Experimental realization of einstein-podolsky-rosen-bohm Gedankenexperiment : A new violation of bell's inequalities, Phys. Rev. Lett. 49, 91 (1982).
[2] A. Zeilinger, https://www.worldscientific.com/doi/10.1142/9789812773210_0006.
[3] N. Fabre, A. Keller, and P. Milman, Time and frequency as quantum continuous variables, Phys. Rev. A 105, 052429 (2022).
[4] E. Descamps, N. Fabre, A. Keller and P. Milman, Quantum metrology using time-frequency as quantum continuous variables: sub shot-noise precision and phase space representation, arXiv 2210.05511 (2022).
[5] T. Douce, A. Eckstein, S. P. Walborn, A. Z. Khoury, S. Ducci, A. Keller, T. Coudreau, and P. Milman, Direct measurement of the biphoton Wigner function through two-photon interference, Scientific Reports 3, 3530 (2013).
[6] N. Fabre, M. Amanti, F. Baboux, A. Keller, S. Ducci and P. Milman, The Hong–Ou–Mandel experiment: from photon indistinguishability to continuous-variable quantum computing, EPJD 76, 196 (2022).

Tunneling Process of Symmetrical State – Phase-space Approach Based on the Time Evolution of the Wigner Distribution Function

Maciej Kalka[1], Dariusz Woźniak[1], Marta Wleklińska[1], Damian Kołaczek[2], Maciej Wołoszyn[1] and Bartłomiej J. Spisak[1]

[1]*AGH University of Science and Technology,*

Faculty of Physics and Applied Computer Science,

al. Mickiewicza 30, 30-059 Kraków, Poland

[2] *University of Agriculture in Kraków, Department of Applied Mathematics,*

ul. Balicka 253c, 30–198 Kraków, Poland

bjs@agh.edu.pl

The Wigner distribution function phase-space formulation of quantum mechanics has widespread applications, including quantum computing, quantum optics, quantum electronics or entanglement [1]. Furthermore, this approach is actively used in theoretical research on the tunnelling effect [2-3]. In Ref. [3], the Wigner function of defected Schrödinger cat states was introduced and its time evolution in the above-barrier regime for a Gaussian potential barrier was analyzed. In this work the dynamics of a symmetrical quantum state constructed of a coherent superposition of well-separated Gaussian wave packets is analyzed with a focus on the effect of *double-sided* barrier penetration by Gaussians moving in opposite directions (see Fig. 1). Three families of quantum states are discussed in consequence of the changes in the relative phase of superposition: even and odd Schrödinger cat states, and Yurke-Stoler states (see Fig. 2). To describe the quantum dynamics, the phase-space entropic measure is introduced and its relation to the nonclassicality parameter [4] is presented. The lower bound of the entropic measure is established in such a way that it corresponds to the Heisenberg uncertainty principle. Moreover, using symplectic invariance of the proposed dynamical characteristics, it is shown that the time of the interaction with the potential barrier can be studied using Wigner function, and that the respective symplectic approach to the *tunneling time* is comparable to the mean flight time considered by Pollak et al. [5].

[1] J. Weinbub and D. K. Ferry, Appl. Phys. Rev. **5**, 041104 (2018)

[2] M.S. Marinov and B. Segev, Phys. Rev. A **54**, 4752 (1996)

[3] D. Kołaczek, B. J. Spisak and M. Wołoszyn, Sci. Reports **11**, 11619 (2021)

[4] A. Kenfack and K. Zyczkowski, J. Opt. B Quantum Semiclassical Opt. 6, 396 (2004)

[5] E. Pollak, Phys. Rev. Lett. **118**, 70401 (2017)

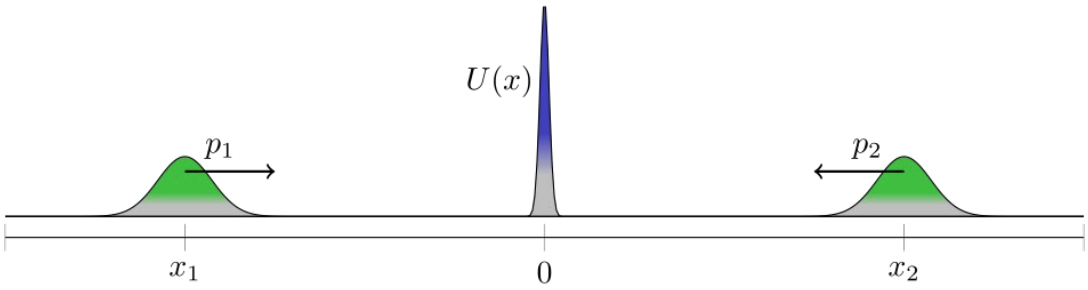

Fig.1: Conceptual design of the symmetrical quantum state approaching symmetrical potential barrier in the shape of Gaussian repulsive potential.

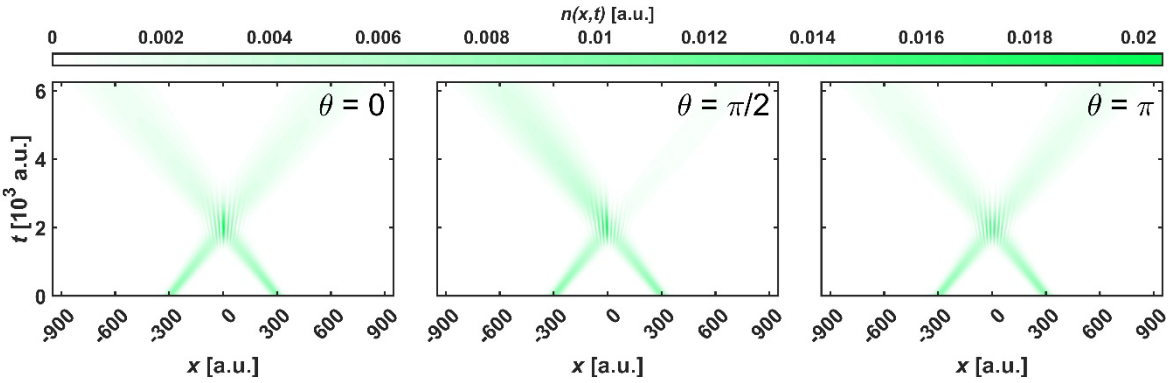

Fig.2: Influence of the relative phase θ on the probability density in real space n(x,t), for the Gaussian potential barrier localized at 0 a.u.; for the even Schrödinger Cat state: $\theta = 0$, for the Yurke-Stoler state: $\theta = \pi/2$, and for the odd Schrödinger Cat state: $\theta = \pi$.

Correlation Functions in Calogero Sutherland Model

Grigory E. Astrakharchik[1,2], Andrea Colcelli, and Andrea Trombettoni[1]

[1] *Department de Fìsica, Universitat Politècnica de Catalunya, Campus Nord B4-B5, E-08034, Barcelona, Spain*

[2] *Departament de Fìsica Quàntica i Astrofisica, Facultat de Fìsica, Universitat de Barcelona, E-08028 Barcelona, Spain*

[3] *Dipartimento di Fisica - Strada Costiera, 11, I-34151 Trieste, Italy*

grigori.astrakharchik@upc.edu

The Calogero-Sutherland model (CSM) is a one-dimensional quantum mechanical model describing a system of interacting particles with inverse-square pairwise interactions, commonly denoted as $\lambda(\lambda-1)/x^2$ where λ is a dimensionless parameter. The ground-state wave function of a trapped system is known exactly and has Laughlin-type form, $\psi= \Pi_{i<j} \exp(-x_i^2)|x_i - x_j|^{\lambda}$, where x_i are particle positions. The energy levels of the Calogero-Sutherland model are known to be closely related to the eigenvalues of certain random matrices, such as the Gaussian Unitary Ensemble (GUE), Gaussian orthogonal ensemble (GOE), and Gaussian symplectic ensemble (GSE) described by different values of λ, which corresponds, apart from a factor 2, to the Dyson index in Random Matrix Theory. The density profile for large number of particles corresponds to the shape of the Wigner semicircle distribution, $n(x)=2/(\pi R^2)\cdot(R^2-x^2)^{1/2}$, where R is the Thomas-Fermi size. We study the pair distribution function, which provides the probability of finding to particles separated by a certain distance in the quantum mechanical model and can be mapped to the level spacing distribution of Random Matrices, with the mapping known as Wigner surmise. We use Monte Carlo algorithm to find the properties numerically. As well, we calculate the one-body density matrix both for bosonic and fermionic statistics of the particles. Natural orbital analysis provides information on the occupation of the eigenstates of the OBDM and is related to the phenomenon of Bose-Einstein condensation in the bosonic case. We provide approximate expressions for the correlation functions.

[1] B. Sutherland, Phys. Rev. A **4**, 2019 (1971).

[2] F. Calogero, J. Math. Phys. **10**, 2191 (1969).

[3] B. Sutherland, Beautiful models, World Scientific, Singapore, 2004.

[4] D. M. Gangardt and A. Kamenev, Nucl. Phys. B **610**, 578 (2001).

[5] G. E. Astrakharchik, D. M. Gangardt, Yu. E. Lozovik, and I. A. Sorokin, Phys. Rev. E **74**, 021105 (2006).

[6] A. Colcelli, G. Mussardo, and A. Trombettoni, EuroPhys. Lett. **122**, 50006 (2018).

[7] J. Dubail, J.-M. Stéphan, J. Viti, and P. Calabrese, SciPost Phys. **2**, 002 (2017).

ISBN: 978-3-95047-385-8